Dynamic Modeling and Control of a Fluidized Bed Reactor for the Oxidative Dehydrogenation of Ethylbenzene to Styrene

Abdelhamid Ajbar and Emaddine Ali[1]
Department of Chemical Engineering, King Saud University
P.O.Box 800, Riyadh, 11421, Kingdom of Saudi Arabia

Abstract. A dynamical model is proposed for a fluidized bed catalytic reactor for the production of styrene by oxidative dehydrogenation of ethylbenzene. A parametric sensitivity analysis carried out previously showed the feasibility of the fluidized bed technology to produce styrene in the reactor on a continuous basis. The static and dynamic bifurcation of the reactor model carried out in this paper shows that the reactor is to be operated in a multiplicity region in order to yield a maximum production rate of styrene. A model predictive control strategy is used with the proposed dynamic model for the tight control of the reactor. The performances of the control algorithm are illustrated for both perfect and imperfect models.

Nomenclature

A	Reactant in the chemical reaction $A \rightarrow B$
A_b	Cross-sectional area of bubble phase
$\hat{A}$	Linear constraints matrix
b	Vector of lower and upper bounds of the linear constraints
B	Product in the chemical reaction $A \rightarrow B$

---

[1] Corresponding author: E-mail:f45k026@ksu.edu.sa, Fax:++(9661)467-8770

C_j	Concentration of component j, (gmole/m³)
C_{js}	Surface concentration for the active site occupied by component j, (gmole/gcatalyst)
C_m	Total concentration of the active site
Cp_g, Cp_s	Specific heats of gas and catalyst, respectively, (J/kg K)
H	Expanded bed height, (m)
$(H_{bd})_b$	Interphase heat transfer coefficient between bubble and dense phase , (J/m³ s K)
$(K_{bd})_b$	Interphase mass transfer coefficient between bubble phase and dense phase, (s⁻¹)
K_j	Adsorption equilibrium constant for component j, (m³/gmole)
Le_i	Lewis number for component i
M	Control horizon
N_{jb}	Molar flow rate of component j in the bubble phase, (gmole/s)
N_{jd}	Molar flow rate of component j in the dense phase, (gmole/s)
$(N_{jF})_b$	Molar flow rate of component j at the inlet of the bubble phase, (gmole/s)
$(N_{jF})_d$	Molar flow rate of component j at the inlet of the dense phase, (gmole/s)
N_{jF}	Total molar flow rate of component j in the fresh feed to the reactor, (gmole/s)
n_y	Number of controlled outputs
P	Output prediction horizon
Q_F	Volumetric flow rate of total feed to the reactor, (m³/s)
Q_b	Volumetric flow rate of bubble phase, (m³/s)
Q_d	Volumetric flow rate of exit dense phase, (m³/s)
r	Set point for the controlled variable
r_i	Kinetic rate for reaction i, (gmole/s gcatalyst⁻¹)
t	Time, (s)
t_k	Time at sampling instant k
T_b	Bubble phase Temperature, (K)
T_d	Dense phase Temperature, (K)
T_F	Feed gas Temperature, (K)
T_{ref}	Reference Temperature, (K)
u	Manipulated variable vector
u_b	Superficial velocity of bubble phase gas, (m/s)
V	Overall volume of reactor, (m³)
x	State vector
X	Active site

y	Model output vector
z	Distance along bed height, (m)

Greek letters

α_I	$= \dfrac{(K_{bd})_{jb}}{u_b}$
α_{ij}	Stoichiometric coefficient of component j in reaction i
β	$= \dfrac{H_{bd}}{u_b \rho_g Cp_g}$
ΔH_I	Heat of reaction i, (J/gmole)
ΔU	vector of M future manipulated variable change
ε	Bed voidage
Γ	Diagonal weight matrix on the predicted error
Λ	Diagonal weight matrix on the manipulated variable
ρ_g	Gas density, (kg/m^3)
ρ_p	Solid particle density, (kg/m^3)
Φ_j	Mass capacity of component j
Φ_h	Dimensionless heat capacity for dense phase

Introduction

The successful industrial applications of some oxidation processes such as oxyclochrination and ammoxidation have revived interest in the oxidative dehydrogenation processes. The oxidative dehydrogenation process has been for instance used successfully [1] on a commercial basis for butadiene production in a fixed bed reactor. Another important candidate is the production of styrene from ethylbenzene. Elnashaie *et al.* [2] have investigated in a previous paper the applicability of the fluidized bed technology to the production of styrene by the oxidative dehydrogenation route. The fluidized bed technology is known in some cases to provide better performances than the conventional tubular reactor. Poor diffusion limitations associated with the use of porous catalyst pellets common in fixed beds, do not exist in fluidized beds because of the generally small sizes of the catalyst pellets used in fluidized bed reactors. Efficient mixing in a bubbling fluidized bed reduces also the risk of the development of hot spots and makes it possible to operate the reactor at the desired optimum operating temperature, where tubular reactors are characterized by temperature profiles along the length of the reactor. The preliminary

investigation carried out by Elnashaie *et al.* [2] has shown that fluidized bed can be used efficiently on a continuous basis for the production of styrene under adiabatic conditions. The objectives of this paper are two fold. The first objective is to develop a dynamic model of the non-isothermal fluidized bed catalytic reactor. For this purpose a lumped parameter adsorption-desorption equilibrium model is first developed for the catalyst pellet. A steady state optimization is then carried out to find the optimum operating conditions for the reactor. In the second stage the static and dynamic bifurcation of the reactor model are investigated. The results of the bifurcation analysis show that the reactor is to be operated in a multiplicity region. A control algorithm is then required to prevent the reactor from drifting towards the low temperature (quenched) steady state or the high temperature (burn out) steady state. The second objective of this paper is to study the control of the unit through the use of a nonlinear model predictive control strategy. The effects of modeling errors, that arise mainly from imperfect knowledge of kinetic rates are also taken into consideration.

Process Model

A rigorous mathematical model of the fluidized bed reactor using the two-phase theory of fluidization [3] is used for the modeling of the unit. The two-phase model which considers the reactor as consisting of a bubble phase and a surrounding dense phase has proved to be the most suitable model of the many models proposed in the past, for incorporating recent findings on the hydrodynamics of fluidization [4]. A review of the relevant models in the literature [5] showed that generally most investigators accept the division of flow into two phases but differ in the detailed description such as the nature of the bubble phase, interphase transfer and flow patterns in the two phases.

A large number of steady state models for isothermal fluidized bed catalytic reactors exist in the literature. A useful review of most of these models can be found in the special topic issue of "Chemical Engineering Research Design" dedicated to John F. Davidson [6]. Despite the abundance of isothermal steady state models there are relatively few non-isothermal dynamic models for these reactors. In addition some of the non-isothermal dynamic models proposed in the literature ignore the importance of bubbles [7], and instead consider the mass and heat transfer resistance between the gas-phase and the solid particles. These resistance are generally negligible because of the small particle sizes used in fluidized beds, in addition to the solid and gas flow conditions in these reactors. Another important factor in the dynamic modeling of the fluidized bed reactors is the importance of the adsorption capacity of the solid catalyst in the dense phase. While not affecting the steady state behavior of the reactor model, the adsorption capacity can have important effects on the dynamic characteristics of the model [8]. Elnashaie and coworkers [9-11] have proposed a model for the non-isothermal fluidized bed catalytic reactor that takes into account the effect of bubbles and the effects of the adsorption capacity. The model was used successfully to analyze and represent the steady state and dynamic behavior of type IV industrial fluid

catalytic cracking units [12-14]. The model has been also used by Choi and Ray [15] to model and control industrial polyethylene reactors. The basic assumptions of the model are:

- The gas in the bubble phase is assumed to be in plug flow.
- The extent of reaction in the bubble cloud phase is negligible. This assumption is justified by the experimental evidence of Torr and Calderbank [16] for small particles (less in size than 150 μm) and high flow rates giving rise to fast rising large bubbles and negligible cloud phase.
- The dense gas phase is assumed to be perfectly mixed. Important evidence shows perfect mixing is approached when the gas is strongly adsorbed on the solid.
- Negligible mass and heat transfer resistances are assumed between the solid particles and the dense phase gas.
- No radial or axial variations of temperature in the dense phase.
- An average value of the bubble size and hence an average value for the exchange parameter is used for the whole bed, an assumption which was validated [17].
- Negligible heats of adsorption.

Bubble phase balance equations
Because of the relatively high heat and adsorption capacities of the solid in the dense phase, the bubble phase can be assumed to be in pseudo-steady state. This assumption allows to write pseudo-steady state mass and heat balance equations for the bubble phase.

Mass balance equations
The mass balance equation for the j_{th} component over a small element of height dz shown in Fig. 1 gives:

$$\frac{dN_{jb}}{dz} = (K_{bd})_{jb}(\frac{N_{jd}}{Q_d} - \frac{N_{jb}}{Q_b})A_b \tag{1}$$

where the N_{jb}, N_{jd} are the number of moles of the component j respectively in the bubble and dense phase, Q_d and Q_b the (corresponding flow rates and K_{bd} is the mass transfer coefficient between the two phases. 1)

Integrating this equation from initial feed conditions $N_{jb} = (N_{jF})_b$ at z = 0 yields

$$(\frac{N_{jb}}{Q_b} - \frac{N_{jd}}{Q_d}) = (\frac{(N_{jF})_b}{Q_b} - \frac{N_{jd}}{Q_d}) e^{-\alpha_j z} \tag{2}$$

where

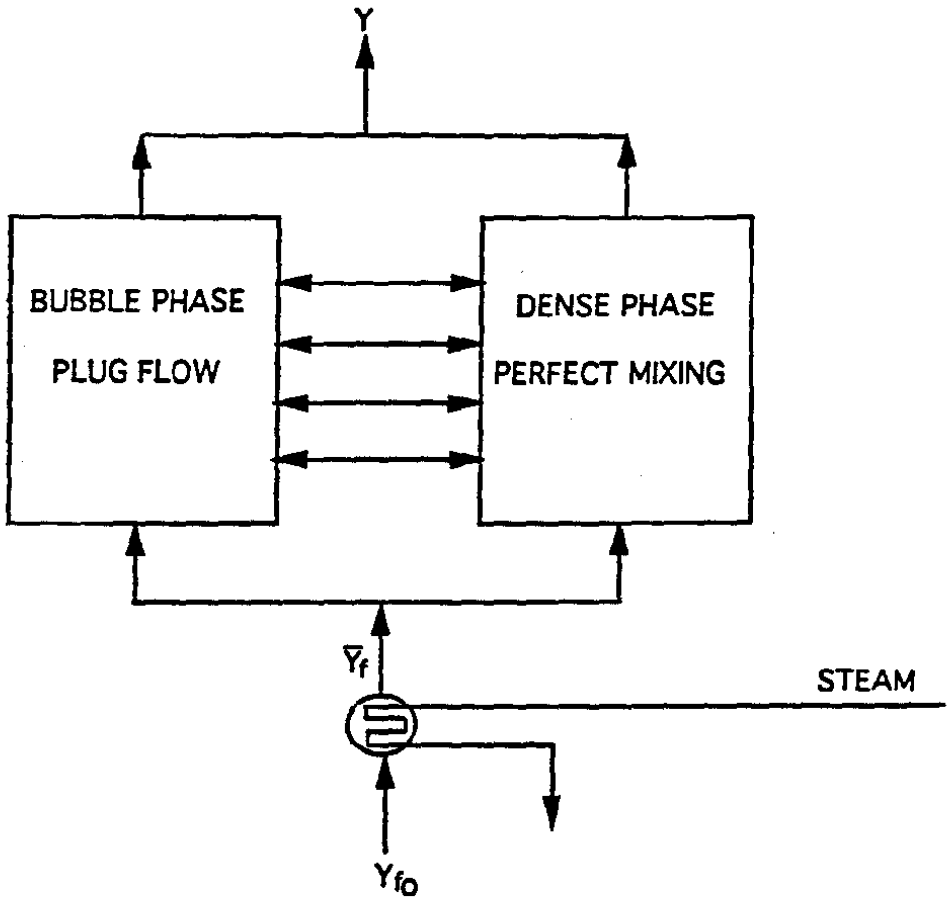$$\alpha_j = \frac{(K_{bd})_{jb}}{u_b}$$

Fig.1. Schematic diagram of the two-phase fluidized bed reactor.

and $u_b = Q_b/A_b$ is the superficial gas velocity of bubble phase.
Noting that

$$\frac{(N_{jF})_b}{Q_b} = \frac{N_{jF}}{Q_F} \tag{3}$$

Equation (2) is also equivalent to

$$(\frac{N_{jb}}{Q_b} - \frac{N_{jd}}{Q_d}) = (\frac{N_{jF}}{Q_F} - \frac{N_{jd}}{Q_d})\, e^{-\alpha_j z} \tag{4}$$

Energy balance equations

Similarly an energy balance over the height dz in the bubble phase gives

$$\rho_g Cp_g u_b \frac{dT_b}{dz} = H_{bd}(T_d - T_b) \tag{5}$$

where H_{bd} is the heat transfer coefficient between the two phases. Integrating this equation from initial feed temperature ($T_b = T_F$ at $z = 0$) yields

$$T_b = T_d - (T_d - T_F) e^{-\beta z} \tag{6}$$

where $\beta = \dfrac{H_{bd}}{u_b \rho_g Cp_g}$

Dense phase balance equations

Mass balance equations

The mass balance for the j_{th} component in the dense phase can be written as

$$N_{jd} = (N_{jF})_d + \int_0^H (K_{bd})_{jb} (\frac{N_{jb}}{Q_b} - \frac{N_{jd}}{Q_d}) A_b dz + V(1-\delta)(1-\epsilon)\rho_p \sum_{i=1}^{3} \alpha_{ij} r_i$$

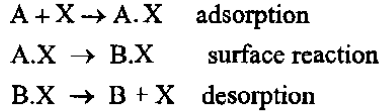$$+ V\epsilon \frac{dC_j}{dt} + V(1-\epsilon)\rho_s \frac{dC_{js}}{dt} \tag{7}$$

where

- C_{js} (gmole gcatalyst^{-1}) is the surface concentration of the active sites occupied by component j.
- V is the bed volume
- r_i (gmole gcatalyst^{-1} s^{-1}) is the rate of reaction for component i
- α_{ij} are the stoichiometric coefficients (negative for the reactants, positive for products and zero for components not appearing in the reaction).

The accumulation term $V\epsilon \dfrac{dC_j}{dt} + V(1-\epsilon)\rho_s \dfrac{dC_{js}}{dt}$ represents the mass capacity for

component j. This term could be simplified by expressing the surface concentration C_{js} in

terms of the gas-phase concentration C_j. The resulting relation is however quite complicated

in the general case and can overshadow the practical side of the model. To circumvent the

need for using non-linear complicated isotherms we will be guided by the case of the simple catalyzed reaction

$$A \to B$$

with the following commonly assumed steps

$$A + X \to A.X \quad \text{adsorption}$$
$$A.X \to B.X \quad \text{surface reaction}$$
$$B.X \to B + X \quad \text{desorption}$$

where X denotes an active site. Assuming that the adsorption-desorption processes are so rapid compared to the rate of the surface reaction so that the net rate of adsorption-desorption can be considered at equilibrium then it is known [18] that the surface concentration of the active site C_{js} can be written as

$$C_{js} = \frac{K_j C_j C_m}{1 + K_A C_A + K_B C_B} \tag{8}$$

where the K_j (m³/gmole) is the adsorption equilibrium constant for component j, and C_m is the total concentration of the active sites. A simplified linear relation for the C_{js} can be obtained by neglecting the term $\sum_{i=1}^{2} K_i C_i$, a valid assumption in the case of a dilute system. The resulting linearized equilibrium adsorption-desorption relation is then

$$C_{js} = K_j C_j C_m \tag{9}$$

resulting in a linear relation

$$\frac{dC_{js}}{dt} = C_m \frac{d(K_j C_j)}{dt} \tag{10}$$

This simple example shows that the resulting relation for the general case of simultaneous reactions, as in the problem treated in this work will be obviously more complicated. The model is also further complicated by the fact that the equilibrium constant is temperature dependent. Accounting for the explicit dependence on the temperature will also cause much complexity in the derivation.

A useful and more practical approach to be taken in the modeling of the mass capacity

is to assume a linear equilibrium adsorption-desorption relation similar to Eq. 9 and to consider the equilibrium constant to be temperature insensitive, or to take it as an average value over the range of temperature covered for the investigation. In order to account for the neglected dynamics the mass capacity for each component is then treated as a bifurcation parameter for the model. The available numerical techniques for continuation algorithms [19] allow the investigation of effects of the mass capacity on the dynamic characteristics of the reactor for a wide range of the parameter values.

Define then

$$\phi_j = \varepsilon + (1-\varepsilon)\rho_j K_j C_m \tag{11}$$

as the effective mass capacity for component j. The base (nominal) values of the adsorption capacities for ethylbenzene, oxygen and styrene can be computed from the kinetics rate k_1, k_2 and k_3 given in the appendix. As mentioned previously an average value over the temperature range [298 K, 1000 K] is taken for the k_j. For the rest of products, i.e., carbon dioxide and water vapor the adsorption capacities are neglected and the mass capacity for the two products is reduced to the bed porosity.

Substituting Eq. 10 in Eq. 7, the mass balance equation in the dense phase can be written as

$$\phi_j \frac{V}{Q_d} \frac{dN_{jd}}{dt} = N_{jd} - N_{jdF} - \int_0^H (K_{bd})_{jb}(\frac{N_{jb}}{Q_b} - \frac{N_{jd}}{Q_d})A_b dz + V(1-\delta)(1-\varepsilon)\rho_p \sum_{i=1}^3 \alpha_{ij} r_i \tag{12}$$

The integral in Eq. 12 can be evaluated analytically by using the corresponding mass balance of Eq. 4. The mass balance equation of the dense phase becomes then

$$\phi_j \frac{V}{Q_d} \frac{dN_{jd}}{dt} = N_{jdF} - (\frac{N_{jF}}{Q_F} - \frac{N_{jd}}{Q_d})u_b A_b(1-e^{-\alpha_j H}) - V(1-\delta)(1-\varepsilon)\rho_p \sum_{i=1}^3 \alpha_{ij} r_i \tag{13}$$

Energy balance equations

The unsteady state heat balance in the dense phase assuming adiabatic conditions can be written as follows

$$\rho_g Cp_g Q_{dF}(T_F - T_{ref}) + \int_0^H (H_{bd})_b(T_b - T_d)A_b dz + V(1-\delta)(1-\varepsilon)\rho_p \sum_{i=1}^3 (-\Delta H_i) r_i =$$

$$\rho_g Cp_g Q_d(T_d - T_{ref}) + V(1-\varepsilon)\rho_s Cp_s \frac{dT}{dt} \tag{14}$$

The integral in Eq. 14 can be evaluated analytically using Eq. 6. Equation 14 yields then:

$$V(1-\varepsilon)\rho_s Cp_s \frac{dT}{dt} = \rho_g Cp_g Q_{dF}(T_F - T_{ref}) + V(1-\delta)(1-\varepsilon)\rho_p \sum_{i=1}^{3} (-\Delta H_i)r_i$$
$$- \rho_g Cp_g Q_d(T_d - T_{ref}) + u_b A_b \rho_g Cp_g(T_F-T_d)(1-e^{-\beta H}) \qquad (15)$$

The term $(1-\varepsilon)\rho_s Cp_s$ can be rendered dimensionless by defining the heat capacity ϕ_h of the dense phase as

$$\phi_h = \frac{(1-\varepsilon)\rho_s Cp_s}{\rho_f Cp_f} \qquad (16)$$

The effects of both mass and heat capacities can be lumped by defining the Lewis number Le_j for each component j as the ratio of the heat capacity to the mass capacity i.e.

$$Le_j = \frac{\phi_h}{\phi_j} \qquad (17)$$

The lewis numbers while not affecting the steady state behavior of the system can have profound effect on the dynamic characteristics of the system [8]. For liquid phase reactors the lewis numbers will almost often be close to unity. For gas solid catalytic reactors like the one studied in this work the mass capacity of a strongly chemisorbed component may exceed the heat capacity and the Lewis numbers may both vary from unity. Dynamic models which assume negligible chemisorption capacities of the different components on the catalyst result in very large values of the Lewis numbers and therefore the mass balance equations predict extremely fast responses for the concentrations compared with the response of the temperature given by the energy balance. Under these physically questionable assumptions the system becomes dynamically one dimensional (in temperature) and most of the dynamic characteristics of the system are lost.

Optimization and Bifurcation Analysis

Equations (13,15) represent the unsteady state model of the reactor involving the six unknowns: the molar flow rates of the five components and the temperature of the dense phase. The hydrodynamic and transport property correlations were given by [1]. The dynamic model includes a large number of parameters. Some of them are pertinent to the

hydrodynamics of the bed while some others can be considered as operating parameters. In the first stage a meaningful set of operating parameters is selected and a steady state optimization is carried out. The selected operating parameters are the feed temperature T_F, the ratio of air to ethylbenzene and the feed flow rate Q_F The styrene production rate is chosen as the objective function to maximize. The production rate is defined as the sum of the molar flow rate of styrene $(N_{st})_b$ in the dense phase and in the bubble phase $(N_{st})_b$. The optimization problem is then to maximize the production rate of styrene subject to the constraints imposed by the steady-state equations of the model. Additional constraints are added to the optimization problem. An upper constraint on the dense phase temperature is set at 820 K as dictated by the practical upper limit on the operating parameters [690K, 820 K] below which the reported kinetics are valid [20]. Because the boiling point of ethylbenzene (which is the component with the highest boiling point in the system) is 409.2 K, the feed temperatures for the gas fluidized bed reactors must be greater than 409.2 K. The optimization problem is then, formally,

$$\text{maximize } (N_{st})_t = (N_{st})_b + (N_{st})_d$$

subject to

$$0 = N_{jd} - N_{jdF} - \int_0^H (K_{bd})_{jb}\left(\frac{N_{jb}}{Q_b} - \frac{N_{jd}}{Q_d}\right)A_b dz + V(1-\delta)(1-\varepsilon)\rho_p \sum_{i=1}^3 \alpha_{ij} r_i, \quad j = 1,\dots,6$$

$$0 = \rho_g Cp_g Q_{dF}(T_F - T_{ref}) + V(1-\delta)(1-\varepsilon)\rho_p \sum_{i=1}^3 (-\Delta H_i) r_i - \rho_g Cp_g Q_d(T_d - T_{ref}) +$$
$$u_b A_b \rho_g Cp_g(T_F - T_d)(1 - e^{-\beta H})$$

$$T_d \leq 820$$
$$T_F \geq 409.2$$

The unknowns for this optimization problems are the molar follow rates N_{jd} of the six components, the dense phase temperature T_d, the feed temperature T_F, the ratio of air to ethylbenzene and the feed flow rate Q_F (or equivalently, the superficial velocity since the cross sectional area of the bed is fixed). The data used for the optimization is shown in Table 1. The optimization problem is solved using the successive quadratic optimization routine DNCONF provided by the IMSL library [21].

Table 1. Reactor design parameters

Bed height at static operations	2.0m
Bed diameter	4.5m
Static bed voidage	0.4
Bed voidage at minimum fluidization condition	0.4
Catalyst particle size	300μm
Catalyst particle density	3000 kg/m^3

The results of the steady state optimization are summarized in Table 2. The total production rate of styrene is 13.960 (gmole/s) of which 8.648 (gmole/s) are produced in the dense phase. Because of the assumed adiabatic conditions the reactor is to be operated obviously at the maximum allowable temperature of 820 K. The ratio of styrene to air is to be 0.198 and the optimal feed temperature corresponds to the normal boiling point of ethylbenzene. The optimal feed flow rate corresponds to a superficial velocity of 46.98 (cm/ s). The bubbling factor, i.e., ratio of the superficial velocity to the velocity at the minimum fluidization is 5.32, a value which is consistent with the assumed bubbling nature of the bed.

Table 2. Results of the steady state optimization

	In the reactor	In the dense phase
Moles of styrene produced	13.96 gmole/s	8.648 gmole/s
Moles of ethylbenzene consumed	89.263 gmole/s	17.226 gmole/s
Moles of air consumed	52.518 gmole/s	0.35 gmole/s
Moles of carbondioxide produced	1.932 gmole/s	1.068 gmole/s
Moles of water vapor produced	15.167 gmole/s	7.711 gmole/s
Dense phase temperature	————	820 K
Feed temperature	409.2	————
Ratio of oxygen to ethylbenzene	0.198	————
Feed gas superficial velocity	46.98 cm/s	————
Velocity at minimum fluidization	8.82 cm/s	————

Using the computed optimum values of the operating parameters we investigate next the static and dynamic bifurcation of the model. Figure 2 shows the continuity diagram of the system showing the production rate of styrene vs the feed temperature, for the model parameters given in Tables 1 and 2. The diagram features two stable branches connected to a middle unstable plant by two limit points occurring respectively at T_f= 280.20 K and T_f = 557.05 K. The optimum point is located at a feed temperature physically not realizable (smaller than 409.2 K). The effects of the Lewis number on the location of the Hopf point can be seen in a two-parameter continuation diagram showing the loci of the Hopf point. The Lewis numbers, as mentioned before, incorporate the neglected dynamics in modeling the mass and heat capacities of the system. Since the mass capacity of both carbon dioxide and water vapor are assumed negligible the investigation focuses on the effect of the Lewis number of ethylbenzene, oxygen and styrene.

Figures 3 (a-c) show then the locus of the Hopf point corresponding to the Lewis numbers of the three components. The nominal values of the Lewis numbers are respectively
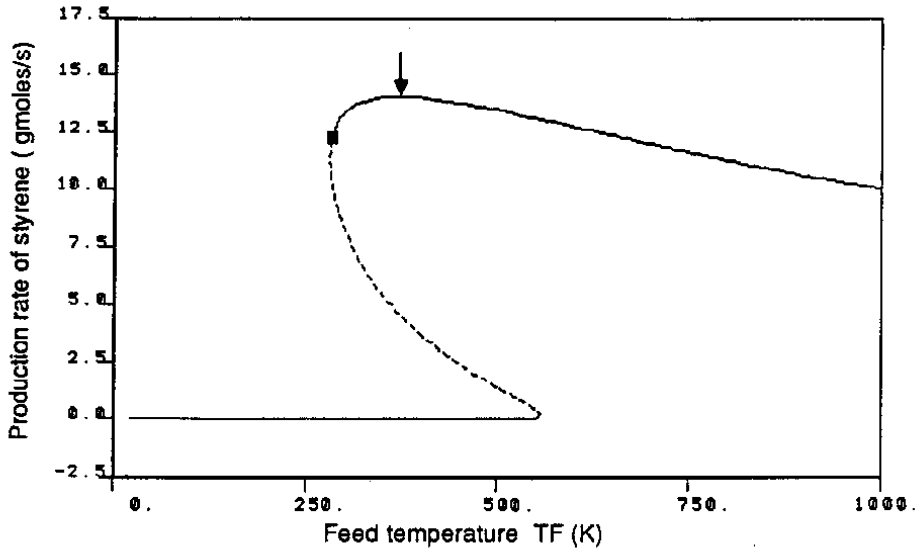
Fig.2. Continuity diagram showing the production rate of styrene Vs the feed temperature. Solid line: stable branch; Dash line: unstable branch; Square: Hopf point. The arrow indicates the desired operation point, giving the maximum production rate.

2.096, 839.56 and 0.717 for ethylebenzene, oxygen and styrene. As mentioned before these values can be computed as an average value of the kinetic rates k_i given in the appendix. The high value of the Lewis number of oxygen indicates a weak chemisorption of the component, as it can be anticipated by comparing the kinetic rates k_i.

It can be seen from Fig. 3 that the feed temperature corresponding to the Hopf point changes only slightly even when the Lewis numbers are varied dramatically around their nominal values. We conclude then that no periodic behavior is expected in the model for the range of physically realizable parameters. The continuity diagram of Fig. 2 corresponds then to the actual situation that can be encountered.

The optimum operating point of Fig.2 although stable, is obviously not globally stable. Variations in the reactor operating parameters could lead the reactor to jump from the high conversion point to the low conversion steady states. A tight control is therefore necessary for the safe operation of the reactor. In the next section the control of the reactor around the optimum operating conditions is investigated.

MPC Algorithm

In this section the structure of MPC version developed by Ali and Zafiriou [22] that utilizes directly the nonlinear model for temperature prediction will be presented. The objective is not to test the Nonlinear MPC (NLMPC) performance through simulation, rather it is to implement
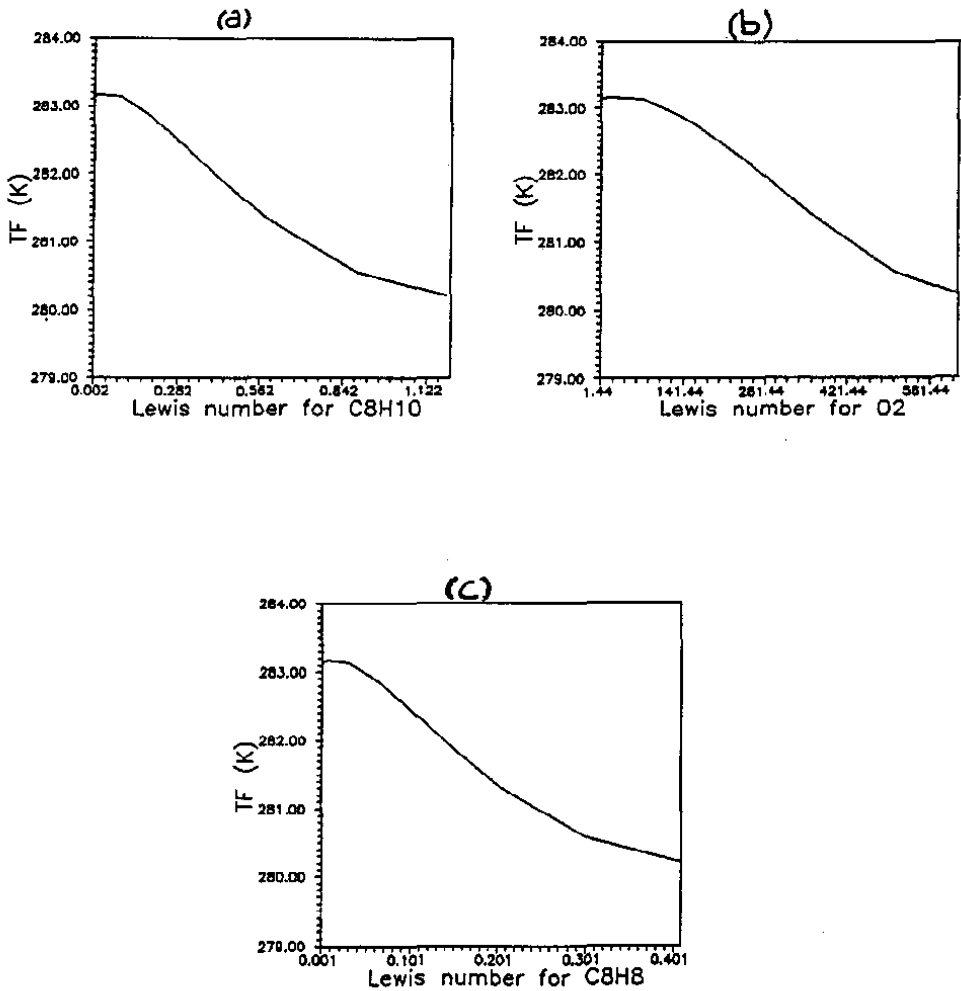
Fig.3. Two-parameter continuation diagram showing the effects of the Lewis numbers on the location of the Hopf point. (a) Effect of the Lewis number for ethylbenzene (b) Effect of the Lewis number for oxygen (c) effect of the Lewis number for styrene.

a controller that can keep the reactor temperature around the desired operating point. This desired operating point was determined by the steady state analysis discussed in the previous section which corresponds to maximum styrene production rate.

A usual MPC formulation solves the following on-line optimization problem:

$$\min_{\Delta u(t_k),\dots,\Delta u(t_{t+M-1})} \sum_{i=1}^{P} \left\| \Gamma(y(t_{k+i}) - r(t_{k+i})) \right\|^2 + \sum_{i=1}^{M} \left\| \Lambda\, u(t_{k+i-1}) \right\|^2 \qquad (18)$$

subject to

$$\hat{A}^T \Delta U(t_k) \le b \qquad (19)$$

For nonlinear MPC the predicted output y over the prediction horizon P is obtained by the numerical integration of:

$$\dot{x} = f(x, u) \qquad (20)$$
$$y = g(x) \qquad (21)$$

from t_k up to t_{k+P}. The symbol $\| \bullet \|$ denotes the Euclidean vector norm and k denotes the current sampling point. Γ and Λ are diagonal weight matrices, r is the desired output trajectories and $\Delta U(t_k) = [\Delta u(t_k) \dots \Delta u(t_{k+M-1})]^T$ is a vector of M future changes of the manipulated variable vector u that are to be determined by the on-line optimization. A disturbance estimate should also be added to y in Eq. 18 or alternatively it can be absorbed in $r(t_{k+1})$. The latter is assumed for simplicity. In this work the disturbance is assumed constant over the prediction horizon, and set equal to the difference between plant and model outputs at present time k. Traditionally, the function of the "additive" constant disturbance in the model prediction is to introduce integral actions and thus remove steady state offset in the face of model uncertainty or unmeasured disturbances.

For our specific case, the state equations (Eq. 20) are the differential equations (Eqs. 13 and 15) developed in section 2. These equations describe the transient behavior of the molar flow rates of five chemical species in addition to the reactor temperature. The measured output of Eq. 21 is taken as the reactor temperature. The definition and the initial values of the states are listed in Table 3. Numerical solution of the differential equations is carried out using DASSL software package [23], and the optimization problems involved in the MPC algorithm are solved using DNCONF routine provided by the IMSL library [21].

Table3. Steady state values of the states

States	Initial	Desired
x_1 (Ethylbenzene)	20.208	17.226
x_2 (Oxygen)	4.012	0.0732
x_3 (Styrene)	————	8.648
x_4 (Carbon dioxide)	————	1.068
x_5 (Water vapor)	————	7.711
x_6 (Temperature)	409.2	820

Closed-loop Simulation Results

The control objective in this paper is to startup the reactor from initial steady state of minimum conversion (quenched state) to a desired steady state of maximum production rate of styrene. Since in practice the composition of the products can not be measured easily, we will, alternatively, use the temperature of the reactor as the controlled variable and the feed temperature as the manipulated variable. The feed temperature is constrained between values of 410 and 650 K. Table 3 lists the values of the sate variables at the initial and the desired steady state points. For robustness purposes, the control objective will also be examined when the model has some degree of parametric uncertainty.

Simulation of NLMPC for setpoint change of magnitude of 410 K in the reactor temperature using sampling time, $T = 1$ s, is shown in Fig. 4. The NLMPC tuning parameters values are $M=5$, $P=20$, $\gamma =10$, and $\lambda =1$. It is found that large value of P, i.e. 20 in this case, enables the controller to stabilize the closed loop response. The figure also shows time-domain response of the styrene molar flow rate (x_3) and the manipulated variable (feed temperature, T_f). Initial substantial increase in the feed temperature is made by the controller which gave enough potential for the reaction to start and the reactor temperature to increase. As the temperature reached its new steady state value, the feed temperature was brought back to its initial value while the reactor temperature is maintained due to the reaction process.

Simulation of the same above control objective for imperfect model is shown in Fig. 5. The model is assumed to possess modeling errors in two of its parameters namely, the activation energy E_1 and E_3 corresponding to the kinetic rates k_1, k_2 and k_3. (The activation energies for k_1 and k_2 are equals, as it can be seen in the appendix). These two parameters were selected because their values are poorly known in general. Fig. 5 shown simulation for a 10% error in the activation energies. Satisfactory results are obtained.

A substantial increase of 30% in the error in the activation energies leads to no reactions at all, thus producing significant model-plant mismatch. Despite this substantial modeling error, the NLMPC was able bring the reactor temperature to the new steady state value of 820 K as it can be seen from Fig.5.
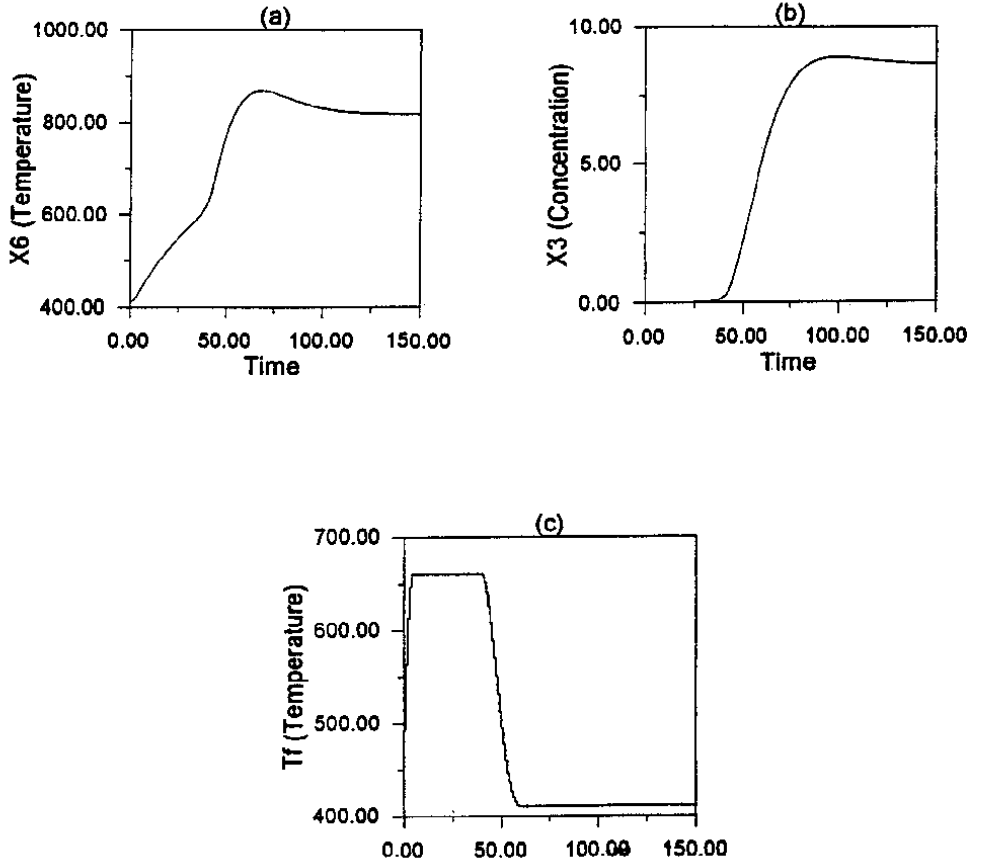
Fig.4. Closed loop response for step change in the reactor set point: The perfect model case. (a) Reactor temperature (b) Concentration of styrene (c) Feed temperature.
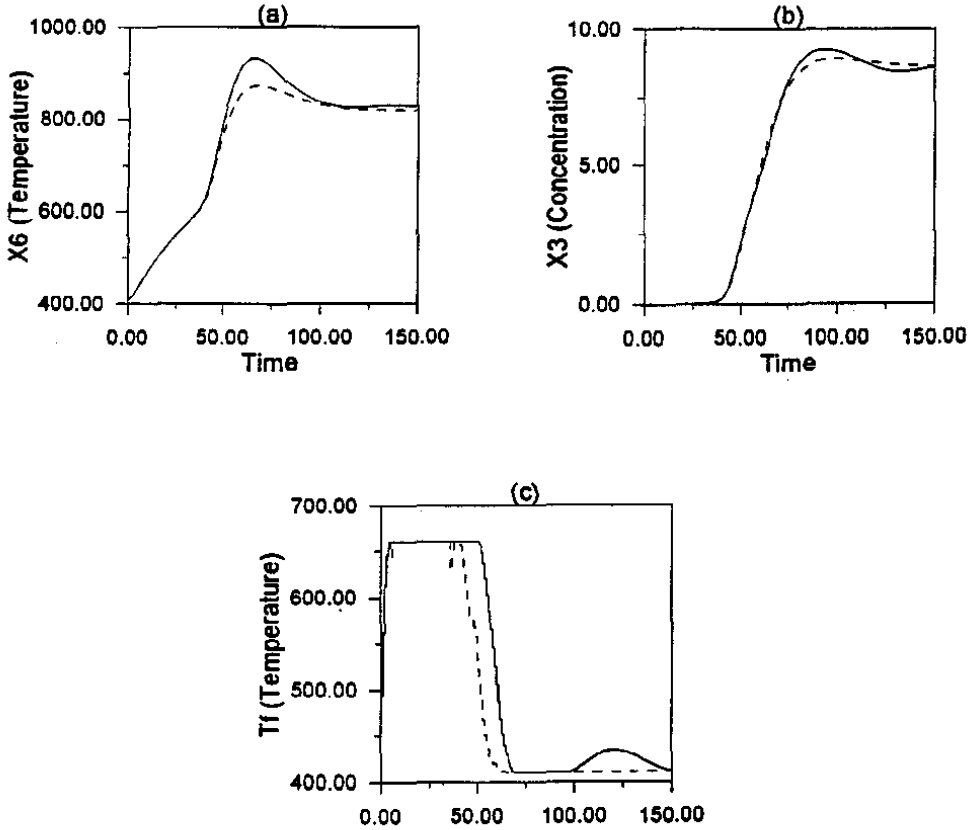
Fig.5. Closed loop response for step change in the reactor set point: The imperfect model case. Solid line: 10 percent error; Dash line: 30 percent error. (a) Reactor temperature (b) Concentration of styrene (c) Feed temperature.

Conclusions

This paper presented a theoretical investigation of the use of fluidized-bed technology for the production of styrene from ethylbenzene by the oxidative dehydrogenation route. A dynamical model based on the two-phase theory of fluidization was used for this purpose. The steady state optimization over the reactor operating parameters shows that a production rate of 13.960 (gmole/s) under adiabatic conditions is possible with an oxygen/ethylbenzene feed ration of 0.198 and a feed temperature of 410 K.

The dynamic investigation shows on the other hand that the maximum operating point is not globally stable. A nonlinear model predictive control strategy was used for the control of the reactor. The NLMPC was effective in handling both the nominal and the robust control cases.
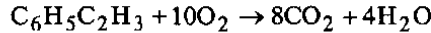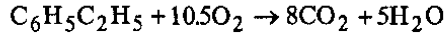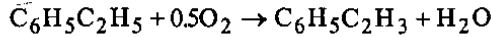
References

[1] Yen, Y.C., Bosch, T. and Styrene, II.V. *SRI Report No. 33A*, 73-102. Menlo Park, California: Stanford Research Institute, 1973.

[2] Elnashaie, S.S.E.H, Wagialla, K.M. and Helal, A.M. "The Use of Mathematical and Computer Models to Explore the Applicability of Fluidized Bed Technology for High Exothermic Catalytic Reactions: II-Oxidative Dehydrogenation of Ethylbenzene to Styrene". *Mathl. Comput. Modelling.*, 15 (1991), 43-54.

[3] Grace, J. R. "High Velocity Fluidized Bed Reactors". *Chem. Engng. Sci.*, 45 (1990), 1953-1966.

[4] Werther, J. "Mathematical Modelling of Fluidized Bed Reactor". *International Chemical Engineering*, 20, No. 4 (1980), 310-315

[5] Yates, J. G. *Fundamentals of Fluidized Bed Chemical Processes*. London: Butterworths, 1983.

[6] *Chemical Engineering Research and Design*. Special Topic Issue: John F. Davidson and Chemical Engineering at Cambridge, 71 (1993), 577-590.

[7] Luss, D. and Amundson, N.R. *Stability of Batch Catalytic Fluidized Beds, AIChE J.*, 14 (1968), 211-215.

[8] Aris, R. *The Mathematical Theory of Diffusion and Reaction in Permeable Catalysts*. 2, 162-167. Oxford: Oxford University Press, 1975.

[9] Elnashaie, S.S.E.H. and Cresswell, D.L. *Dynamic Behavior and Stability of Non-Porous Catalyst Particles, Chem. Engng. Sci.*, 28 (1973a), 1387-1390.

[10] Elnasahie, S.S.E.H and Cresswell, D.L. *On the Dynamic Modeling of Porous Catalyst Particles. Can. J. Chem Engng.*, 51 (1973b), 201-210.

[11] Elnashaie, S.S.E.H and El-Bialy, S. *Multiplicity of the Steady States in Fluidized Bed Reactors V. The Effect of Catalyst Decay. Chem. Eng. Sci.*, 35 (1980), 1357-1367.

[12] Elshishini, S.S. and Elnashaie, S.S.E.H. "Digital Simulations of Industrial Fluid Catalytic Cracking Units. I-Bifurcation and Its Implications". *Chem. Engng. Sci.*, 45 (1990), 553-559.

[13] Elnashaie, S.S.E.H. and Elshishini, S.S. "Digital Simulation of Industrial Fluid Catalytic Cracking Unit. IV. Dynamic Behavior". *Chem. Engng. Sci.*, 48 (1993), 567-571.

[14] Elnashaie, S.S.E.H. and Elshishini, S.S. "Dynamic Modelling, Bifurcation and Chaotic Behavior of Gas-Solid Catalytic Reactors". In: *Topics in Chemical Engineering*. Vol.9; Luxembourg: Gordon and Breach, 1996.

[15] Choi, K.Y. and Ray, W.II. "The Dynamic Behavior of Fluidized Bed Reactors for Solid Catalyzed Gas Phase Olefins Polymerization". *Chem. Engng. Sci.*, 40 (1985), 2261-2279.

[16] Toor, F.D. and Calderbank, P.H. *Proceedings of the Tripartite Chemical Engineering Conference*, London: Inst. of Chemical Engrs., Montreal, Quebec, (1968).

[17] Fryer, C. and Potter, O.E. "Bubble Size Variation in Two-Phase Models of Fluidized Bed Reactors". *Powder Technology*, 6 (1972), .

[18] Carberry, J. J. *Chemical and Catalytic Reaction Engineering*. New York: McGraw-Hill, 1976.

[19] Seydel, R. *From Equilibrium to Chaos: Practical Bifurcation and Stability Analysis*. New York: Elseveier, 1988.

[20] Shakhnovich, G.V, Belomestnykh, I.D, Nekrasov, N.V, Kostyukovsky, M.M. and Kiperman, S.L. "Kinetics of Ethylbenzene Oxidative Dehydrogenation to Styrene Over a Vanadia/Magnesia Catalyst". *Applied Catalysis*, 12 (1984), 23-34.

[21] IMSL. Math/PC-Library, 1985.

[22] Ali, E. and Zafiriou, E. "Optimization-Based Tuning of Nonlinear Model Predictive Control with State Estimation". *J. Proc. Contr.*, 3 (1993), 97-107.

[23] Petzold, L.R. *A Description of Dassl: A Differential-Algebraic System Solver Scientific Computing*, R.S. Stepleman (Ed.). North-Holland, 1983.

Appendix: Reaction Mechanisms and Kinetics

The kinetic model for the oxidative dehydrogenation of ethylbenzene to styrene used in this study was reported by Shakhnovich et al. (1984) and it describes the kinetics on a vanadia/magnesia catalyst. The reaction mechanisms are

$$C_6H_5C_2H_5 + 0.5O_2 \rightarrow C_6H_5C_2H_3 + H_2O$$
$$C_6H_5C_2H_5 + 10.5O_2 \rightarrow 8CO_2 + 5H_2O$$
$$C_6H_5C_2H_3 + 10O_2 \rightarrow 8CO_2 + 4H_2O$$

The rates of oxidation of $C_6H_5C_2H_5$ and $C_6H_5C_2H_3$ according to the above reaction mechanisms are denoted by r_1, r_2 and r_3 and are given by

$$r_1 = K_I \frac{p_{C_8H_{10}} p_{O_2}^{0.5}}{B} \tag{22}$$

$$r_2 = K_{II} \frac{p_{C_8H_{10}} p_{O_2}}{B} \tag{23}$$

$$r_3 = K_{III} \frac{p_{C_8H_8} p_{O_2}}{B} \tag{24}$$

where the r_i are in {gmole/g s}, the partial pressures p_i in kPa and the expression B is given by

$$B = ((1 + k_1 p_{C_8H_{10}} + k_2 p_{C_8H_8} + k_3 p_{O_2})(1 + \alpha \frac{p_{C_8H_{10}}}{p_{O_2}^{0.5}}))^2 \tag{25}$$

The constants K_I, k_i and α have the following values,

$K_I = 4.91 \times 10^{-2} e^{-7100/T}$	{gmole g^{-1} s^{-1} kPa$^{-1.5}$}
$K_{II} = 6.55 \times 10^{-4} e^{-7050/T}$	{gmole g^{-1} s^{-1} kPa$^{-2.0}$}
$K_{III} = 4.55 \times 10^{-3} e^{-7550/T}$	{gmole g^{-1} s^{-1} kPa$^{-2.0}$}
$k_1 = 2.31 \times 10^{-5} e^{6300/T}$	{kPa^{-1}}
$k_2 = 6.71 \times 10^{-5} e^{6300/T}$	{kPa^{-1}}
$k_3 = 2.62 \times 10^{-3} e^{2500/T}$	{kPa^{-1}}
$\alpha = 0.04$	{kPa$^{-0.5}$}

النمذجة الدينامية والتحكم في مفاعل مميع المهد لإنتاج إستيرين من الإثيل

بنزين عن طريق التأكسد النازع للهيدروجين

عبد الحميد أجبار و عماد الدين علي

قسم الهندسة الكيميائية، كلية الهندسة، جامعة الملك سعود، ص ب ٨٠٠،

الرياض ١١٤٢١، المملكة العربية السعودية

(أُستلم في ٢١/١٠/١٩٩٦م؛ وقبل للنشر في ٢٥/٦/١٩٩٧م)

ملخص البحث. يقترح هذا البحث نموذج دينامي لمفاعل محفز مميع المهد لإنتاج الإستيرين من الإثيل بنزين عن طريق التأكسد النازع للهيدروجين. وقد أثبتت دراسة سابقة (النشائي)جدوى تقنية المفاعل المميـــع لإنتـــاج الإستيرين. أظهرت دراسة التشعب الإستاتي والدينامي ضرورة تشغيل المفاعل في منطقة التعددية مـــن أجـل الحصــــول على أقصى إنتاجية من الإستيرين. وقد استعملت طريقة التحكم التنبؤي المبني على النمذجة مـــن أجل التحكم الصارم للمفاعل. وقد تم إبراز أداء نظام التحكم في حالتي النموذج المثالي وغير المثالي.